

# Alternating Current Photovoltaic Module Model

Irtaza M. Syed, Kaamran Raahemifar

**Abstract**—This paper presents modeling of an Alternating Current (AC) Photovoltaic (PV) module using Matlab/Simulink. The proposed AC-PV module model is simple, realistic, and application oriented. The model is derived on module level as compared to cell level directly from the information provided by the manufacturer data sheet. DC-PV module, MPPT control, BC, VSI and LC filter, all were treated as a single unit. The model accounts for changes in variations of both irradiance and temperature. The AC-PV module proposed model is simulated and the results are compared with the datasheet projected numbers to validate model's accuracy and effectiveness. Implementation and results demonstrate simplicity and accuracy, as well as reliability of the model.

**Keywords**—AC PV Module, Datasheet, Matlab/Simulink, PV modeling.

## I. INTRODUCTION

PHOTOVOLTAIC (PV) systems design, simulation, analysis, and optimization require modelling of the system. As one of the core elements, PV module requires realistic and accurate modelling. A model that is simple and yet accounts for variations of parameters such as voltage and current based on irradiance and temperature fluctuations. Traditionally, modules are modelled on cell levels using Shockley equation and one (or two) diode equivalents of PV cells for direct current (DC) systems. However, experience with PV systems and advancements in the PV field resulted in alternating current PV (AC-PV) modules, where micro inverter (MI) integrated DC-PV module is directly applied as AC component.

The literature presents a variety of approaches to model a DC-PV module based on diode equivalent circuit and Shockley equation. References [1]-[5] report one and two diode equivalent circuit models for DC-PV system that require not only the complex physical details of the semiconductor crystalline structure, but also the mathematical details of single or double exponential equations with numerous variables. Additionally, such models are based on the PV cell [not a PV module], require calculation of additional parameters and are meant for DC-PV systems. Sahoo et al. [6] report a one-diode equivalent circuit modeling using Simscape that uses Physical Network, Structural Model, Behavioural Model and Reduced System Equations to derive equations based model for simulation. Liang et al. [7] & Jenifer et al. [8] discuss generalized and mathematical models based on one-diode equivalent circuit and Shockley equation. Again these

Irtaza M. Syed is a student at the Electrical & Computer Engineering Department, Ryerson University, Toronto, ON M5K 2K3 Canada (corresponding author phone: 647-787-6262; e-mail: isyed@ryerson.ca).

Dr. Kaamran Raahemifar, is with the Electrical & Computer Engineering Department, Ryerson University, Toronto, ON M5K 2K3 CANADA, (e-mail: kraahemi@ee.ryerson.ca).

models are on cell level and for DC-PV systems. Sangsawang and Chaitusaney [9] report module level model by modifying one-diode equivalent circuit to derive modified Shockley equation for a PV module. The authors claim the model uses datasheet parameters; however, it requires additional calculation to find parameters not listed in datasheet. Sera et al. [10] follow the work of [9] and focus on finding parameters not listed in datasheet. Farivar and Assaei [11] again loosely follow methods outlined by [9] and [10] while applying additional manipulations. Syed and Yazdani [12] presented PV module modeling on module level directly from datasheet that does not require any manipulation of Shockley equations, diode equivalent circuits, or calculation of extra parameters not listed in datasheet. However, the aforementioned module has also been modeled for DC-PV Systems. This paper presents an approach for modeling AC-PV module that is extracted directly from manufacturer datasheet. The proposed AC-PV module model is simple, requires no additional calculations, and accounts for irradiance and temperature variations. The proposed model shows no significant loss in accuracy and allows simple integration into Matlab/Simulink. The proposed model does not require crystalline structure details and does not use conventional Shockley equation. The model is validated for different irradiance (G) and temperature (T) as an individual module as well as a part of the multiple kW Utility Interactive (UI) PV System. The energy injected into the electric grid is validated to verify the accuracy of the AC-PV model. The rest of the paper is organized into the following sections: (II) PV Systems, (III) AC-PV Module Datasheet, (IV) AC-PV Module Model, (V) Simulation Results, and (VI) Conclusion.

## II. PV SYSTEMS

Based on the type of current at the PV array level, PV systems can be broadly divided into DC-PV and AC-PV systems.

### A. DC-PV System

A DC-PV system consists of a number of DC-PV modules connected in series-string to allow for a useably high DC voltage level and in parallel for higher DC current. This array, series-parallel combination of DC-PV modules, is built until the desired level of DC power is achieved, given by (1) to (3), where  $n_s$  is the number of modules in the string,  $n_p$  is the number of strings in parallel,  $V_s$  is string voltage,  $I_p$  is the net current of strings in parallel,  $V_m$  and  $I_m$  are module voltage and current, and  $P_a$  is the array power.

$$V_s = n_s V_m \quad (1)$$

$$I_p = n_p I_m \quad (2)$$

$$P_a = V_s I_p \quad (3)$$

Then DC-PV array is connected to grid through Maximum Power Point Tracking (MPPT) converter (optional), a DC-link Capacitor, and utility interactive Voltage Source Inverter (VSI). Perturb and Observe (PO) Maximum Power Point Tracking (MPPT) algorithm in conjunction with BC is used to track maximum power point and ensure maximum power delivery. Three phase two level Voltage Source Inverter (VSI) is used to convert DC into AC at 60 Hz and 208 V<sub>LL</sub> volts, compatible with grid (and local load, if any). DC-link capacitor is maintained at specific voltage to ensure stiff voltage at the input of VSI for reliable operation. Fig. 1 shows the DC-PV system.

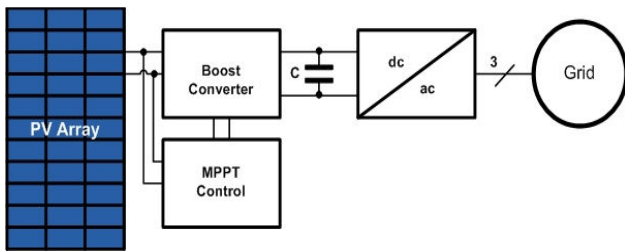


Fig. 1 DC-PV modules PV System

DC wiring expertise is required for proper sizing of the array and installations. The number of modules in a string is usually limited by the system's maximum V<sub>DC</sub> (600V or 1000V); therefore, one usually has to deal with the high voltage on a string level. Also, the current in a series string is defined by and thus depends on the weakest link in the string (module with the lowest current). DC-PV system balance of system (BOS) such as DC fuses, conductors, disconnects, are also required, adding to the system's cost, design complexity and installation time. DC BOS also cause increased power loss. In addition, central VSI results in single point of failure and cannot perform well in areas with shading and soiling (or snow). Output power of the DC-PV system is calculated using (3) and (4), where P<sub>o-dcpv</sub> is the AC output power (or power into the grid) of DC-PV system and d is the de-rating factor, usually 0.75 < d < 0.80. De-rating factor accounts for all the loss from DC-PV array to the grid.

$$P_{o\_dcpv} = dP_a \quad (4)$$

### B. AC-PV System

The NFPA 70 National Electrical Code (NEC) defines an AC module as a complete, environmentally protected unit consisting of solar cells, an inverter and other components, exclusive of a tracking system, designed to produce AC power from the sunlight. AC modules must be evaluated by a nationally recognized testing laboratory using both UL 1741 and UL 1703 as a single unit. Fig. 2 shows AC-PV module. Thus, AC-PV module is a DC-PV module with integrated micro-inverter (MI) that produces AC voltage and current at grid frequency and voltage rather than DC. In an AC-PV module there is no need to size array, no series or parallel

strings, no current mismatch loss, no DC BOS, no DC loss, no shading/soiling/snow issues on one module affecting the others, and no single point of failure. In an AC-PV module we do not have to deal with high voltage and system performance is not partially defined by the weakest link. AC-PV module outperforms the DC-PV due to MI integrated MPPT on a module level rather than string or central level. In an AC-PV module there is no need for transformers or big capacitors and no fan for cooling is required. In addition, factory design, sizing and assembly ensures optimal performance and results in less installation time. Moreover, AC-PV system allows module level monitoring for performance and maintenance. Although AC-PV systems cost more than DC-PV systems, they yield energy improvements of up to 25% and are easier to design and install.

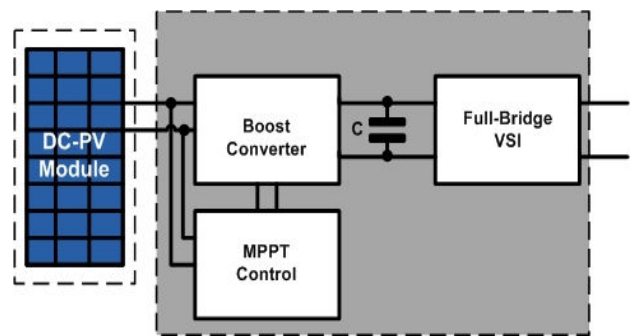


Fig. 2 AC-PV module

An AC-PV system consists of a number of AC-PV modules connected directly across AC system (grid) phases A, B, C and thus all the intermediary steps from PV array to the grid are eliminated. AC-PV modules are wired between two of the three phases. Typically during installation, for each AC-PV module wired between phases A-B, another is wired between phases B-C and yet another between phases A-C (Fig. 3). This installation pattern ensures equal distribution across phases and prevents from imbalance within the 3-phase system. In contrast to DC-PV system, the number of modules in an AC-PV system is limited by the line's current capacity and defines the maximum number of AC-PV modules connected to an AC circuit. The aforementioned will result in 17 (17 x 0.94 ≈ 16A, 16A x 1.25 ≈ 20A) AC-PV modules in a 20A branch circuit. The output power of AC-PV is given by (5), where P<sub>o-acpv</sub> is the AC output power (or power into the grid), n<sub>ui</sub> and P<sub>ui</sub> are the number of MI's and continuous output power of individual AC-PV module, respectively.

$$P_{o\_acpv} = n_{ui} P_{ui} \quad (5)$$

### III. AC-PV MODULE DATASHEET

AC-PV module labels are required to list 6 parameters of AC electrical data (DC-PV modules are required to list 8 key parameters) on their nameplates at Standard Test Conditions (STC) to define their characteristics and performance. STC corresponds to a solar irradiation of 1000W/m<sup>2</sup>, a junction temperature of 25°C, and Air Mass of 1.5. The parameters

listed are the nominal AC operating voltage, nominal frequency, maximum AC current, maximum AC power, branch circuit maximum over current protection device rating, and the number of AC-PV modules that can be attached. Table I tabulates the AC Electrical Data for Sunpower E19/240 AC solar panel.

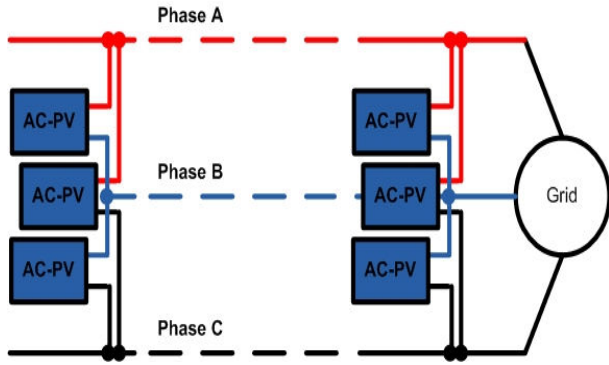


Fig. 3 AC-PV System

In addition to the label listed parameters, Datasheets provide Power Factor, Total Harmonic Distortion, DC electrical data, mechanical data, testing conditions, etc. Table II tabulates DC Electrical Data for Sunpower E19/240 AC solar Panel.

TABLE I  
AC ELECTRICAL DATA OF SUNPOWER E19/240 AC

AC Electrical Data	E19/240 ACPV
AC Output (Min/Nom/Max)	211/240/264 V
Operating $f$ (Min/Nom/Max)	59.3/60/60.5 Hz
Output Power Factor	0.99 Min
AC Max Continuous $I_o$	0.94 A
AC Max Continuous $P_o$	225 W
DC/AC CEC Conversion Efficiency	94.5%
Max Units Per Branch Circuit	17
Max Overcurrent Protection	20 A

As usual datasheets do not provide the series and shunt resistances, diode ideality constant, diode reverse saturation current, and the bandgap energy of the semiconductor. Therefore modeling on cell level using Shockley equation or diode equivalent circuit and on module level that require series/shunt resistances or extra manipulations are not possible. Conventional VI curves are not possible either.

#### IV. AC-PV MODULE MODEL

As pointed out earlier an AC-PV module is the UL certified combination of a DC-PV module and a MI as a single unit (Fig. 2). Therefore, AC-PV module modeling requires models of both DC-PV module and MI.

##### A. DC-PV Module Model

In a DC-PV module, there is a defined relationship between current ( $I_m$ ) and irradiance ( $G$ ) (Fig. 4 and also between module voltage ( $V_m$ ) and temperature ( $T$ ) (Fig. 5). However there is no significant relationship between  $I_m$  and  $T$  or

between  $V_m$  and  $G$ . Therefore, the effects of  $T$  on  $I_m$  and  $G$  on  $V_m$  can be ignored for all practical purposes.

Thus,  $I_m$  as a function of  $G$  at a given instant of  $t$ , is given as:

$$I_{mt} = kI_{STC} \quad (6)$$

where,  $I_{STC}$  = module current at STC;  $G_{STC} = 1000 \text{ W/m}^2$ ;  $G_t = \text{W/m}^2$  at time  $t$ ;  $I_{mt}$  = module current at  $G_t$ ;  $k = G_t/G_{STC}$ .

TABLE II  
DC ELECTRICAL DATA OF SUNPOWER E19/240 AC

DC Electrical Data at STC	E19/240 ACPV
Nominal Maximum Power ( $P_{max}$ )	240 W
Optimum Operating Voltage ( $V_{mp}$ )	40.5 V
Optimum Operating Current ( $I_{mp}$ )	5.93 A
Open Circuit Voltage ( $V_{oc}$ )	48.6 V
Short Circuit Current ( $I_{sc}$ )	6.30 A
Module Efficiency	19.3%
Temperature Coefficients (P)	-0.38%/°C
Temperature Coefficients ( $V_{oc}$ )	-132.5mV/°C
Temperature Coefficients ( $I_{sc}$ )	3.5mA/°C

On the same note, PV module power,  $P_m$  as a function of  $G$  at a given instant of  $t$ , is given by:

$$P_{mt} = kP_{STC} \quad (7)$$

where,  $P_{STC}$  = module power at STC;  $P_{mt}$  = module power at  $t$ .

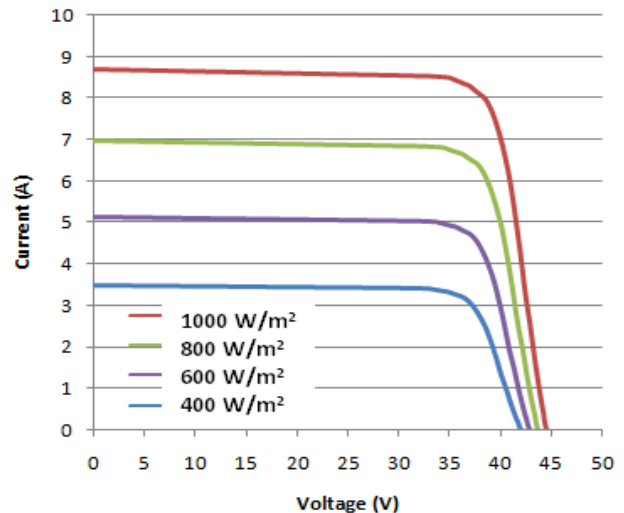


Fig. 4 DC-PV VI curves at different irradiances

Equation (8) is used to account for temperature variations:

$$P_{mT} = [P_{STC}C_p(T_m - T_r)] \quad (8)$$

where,  $C_p$  = module power temperature coefficient;  $T_m$  = module operating temperature;  $T_r$  = module reference (STC) temperature;  $P_{mT}$  = change in module power at temperature  $T$ .

Combining (7) and (8) results in the module behavior with respect to both irradiance and temperature:

$$P_m = P_{mt} + P_{mT} \quad (9)$$

where,  $P_m$  is the module power as a function of both  $G$  and  $T$  at a given instant.

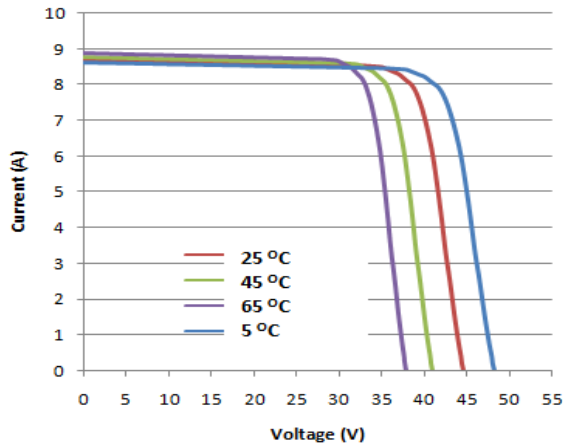


Fig. 5 DC-PV VI curves at different temperature

In a similar way, the PV module voltage as a function of temperature is given by:

$$V_m = V_{OC} + V_{mT} \quad (10)$$

where,  $V_{mT} = V_{OC} C_V (T_m - T_r)$  is module voltage at temperature  $T$ ;  $V_{OC}$  = module open circuit voltage at STC;  $C_V$  = module voltage temperature coefficient.

As pointed out earlier, changes in irradiance do not change the voltage significantly; therefore, changes in  $V$  due to variations in  $G$  are ignored.

Dividing (9) by (10) gives module current ( $I_m$ ) in terms of given  $G$  and  $T$ :

$$I_m = P_m / V_m \quad (11)$$

DC-PV module model based on (9), (10), and (11) is shown in Fig. 6 and can easily be modeled in Matlab/Simulink. All the values for variables in (9), (10), and (11) are obtained directly from DC electrical data of Datasheet.

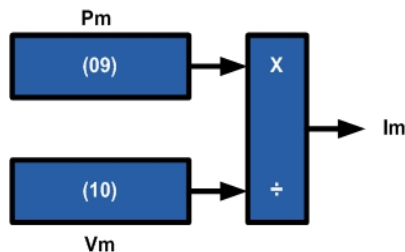


Fig. 6 Proposed model of the DC-PV module

The output of the DC-PV model is converted into current using controlled current source (Fig. 7). Capacitor is used to supply  $V_{in}$  for the BC. Inputs  $G$  and  $T$  are used to model effects of irradiance and temperature across the model.

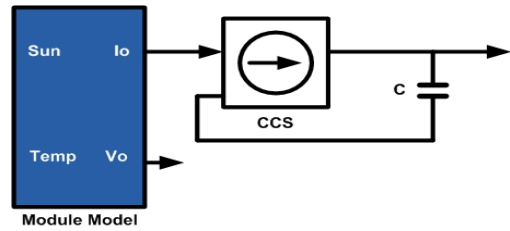


Fig. 7 DC-PV Module Model

### B. Micro-Inverter Model

Both BC and VSI need to be modelled as parts of the DC-PV model to develop a true AC-PV module model. The MI shown in Fig. 2 (the shaded box) is modelled as BC, POMPPT, and a single phase full-bridge (FB) VSI. BC (shaded box) and FB-VSI (dashed box) are shown in Fig. 8.

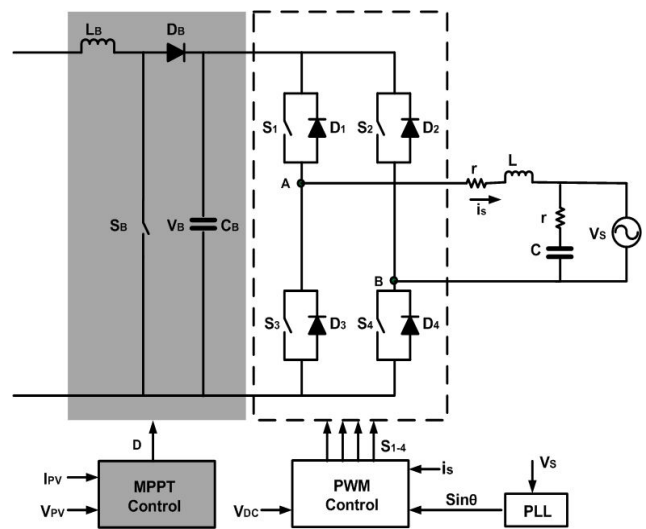


Fig. 8 Micro-Inverter

#### i) PO MPPT Control

Maximum power point ( $P_{mp}$ ), i.e., the point of operation for a DC-PV module with maximum voltage ( $V_{mp}$ ) and maximum current ( $I_{mp}$ ), lies around the knee of the VI curve (Fig. 9).

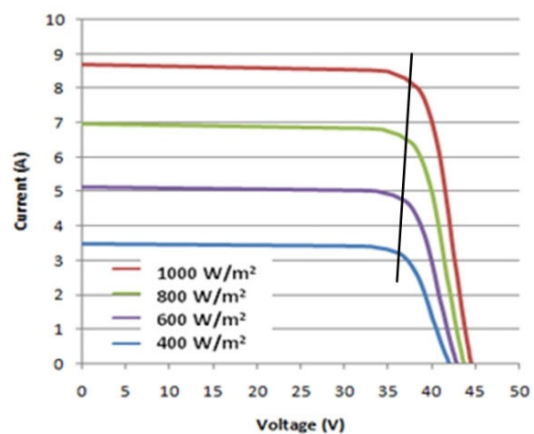


Fig. 9 Maximum power point

Maximum power point is approximated by:

$$V_{mp} = 0.80V_{OC} \quad (12)$$

Depending on the operating conditions such as irradiation and temperature, POMPPT control algorithm continuously adjusts the voltage and current of DC-PV module to ensure  $P_{mp}$  operation. PO algorithm is an iterative process shown in Fig. 10.

The operating point is perturbed (1: present V & I measured & Present P calculated), system response is observed (2: past and present Ps are compared and the direction of the next step/perturbation is determined), (3: based on whether the recent P is greater or less than the previous P). This process mimics the hill-climbing phenomenon to reach the peak of the mountain (maximum power point with  $V_{mp}$  &  $I_{mp}$ ). This way DC-PV module is ensured to operate at mpp.

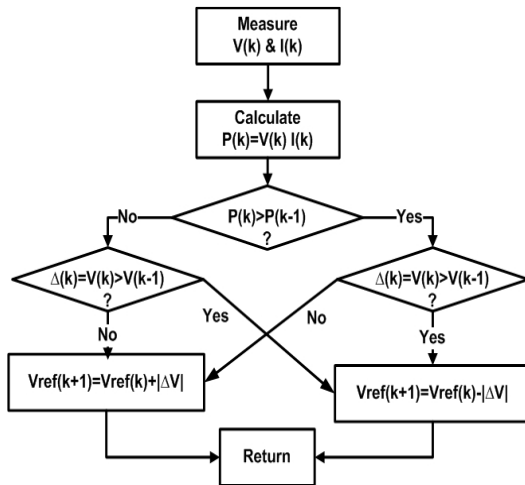


Fig. 10 POMPPT algorithm

### ii) Boost Converter

VSI requires stiff DC voltage equal to or greater than  $\sqrt{2}V_s$  at the input for satisfactory operation (13). However, the output voltage of the DC-PV module depends on the number of series-connected-cells. The output voltage is usually less than 50V and varies with changes in temperature. The output voltage is inversely related to the temperature, i.e., DC-PV module has the highest output voltage for the lowest temperature and the lowest output voltage for the highest temperature. During operation this voltage continuously varies between the two extremes and PO MPPT control supplies  $V_{mp}$  (12) at given irradiance and temperature. Therefore, BC is required to keep voltage fixed at the required level [given by (13)], by varying D, for all the DC-PV voltages between the lowest and the highest. Output voltage of BC is given by (14). D (15) is the duty cycle and can assume any value between 0 and 1. Capacitor C (16) is chosen according to the required amount of output voltage ripple. BC is operated in CCM mode, by choosing L greater than  $L_{min}$  (to ensure  $I_L$  greater than  $I_{LB}$ ) (17).

$$V_{DC} \geq \sqrt{2}V_i \quad (13)$$

$$V_o = \frac{1}{1-D}V_i \quad (14)$$

$$D = \frac{t_{on}}{T} \quad (15)$$

$$C_o = \frac{I_o}{\Delta V_o}DT \quad (16)$$

$$L \geq L_{min} = \frac{T}{2I_{LB}}D(1-D)V_o \quad (17)$$

### iii) Voltage Source Inverter

FB-VSI has four switches and is used to convert DC power into AC power at desired voltage and frequency. The Switches are controlled to adjust the output voltage and frequency, in this case equal to grid voltage and frequency. Anti-parallel diodes are connected across switching devices to allow reverse current flow. VSI requires a stiff DC voltage source at input [1] for quality operation.

The dashed box in Fig. 8 shows a FB-VSI circuit. VSI has two legs each with two switches and two anti-parallel diodes. Leg-1 comprising S1, S3, D1 and D3 (aka Half-Bridge Inverter (HBI)) is the basic building block of this type of inverters. FB-VSI has two HBIs. To ensure proper operation of the bridge and to avoid short circuit no two switches of the same HBI should be turned on simultaneously.

Though output voltage can be controlled by adjusting  $V_{DC}$ , usually the more convenient method of pulse width modulation (PWM) is used. PWM adjusts the pulse width by controlling on and off times of the switches to produce the desired output voltage. In Sinusoidal PWM, the on and off commands for switches are produced by comparing a modulating signal ( $V_{mod}$ ) with a triangular carrier wave ( $V_c$ ) to produce appropriate gating sequence for the switches. Frequency of the carrier wave ( $f_c$ ) is selected adequately higher than the frequency of the modulating signal ( $f_m$ ), usually equal to or greater than 10 times  $f_m$ , for proper operation. The VSI rms output voltage and frequency are determined by  $f_m$  and the amplitude of  $V_{mod}$ , respectively. Both the unipolar (using one carrier wave) and bipolar (using two carrier wave) modulation techniques are employed; however, the latter is preferred due to ease of implementation. Output voltage is given by (18), with  $V_A$  and  $V_B$  given by (19) and (20).

$$V_o = V_A - V_B \quad (18)$$

$$V_A = \left(\frac{t_{on}}{T}\right)V_{DC} \quad (19)$$

$$V_B = \left(\frac{t_{off}}{T}\right)V_{DC} \quad (20)$$

with  $t_{off}$  given by (21) and using (15), (19) and (20), (18) can be re-written as (22). Equation (22) shows that the amplitude of VSI output can be adjusted by varying D.

$$t_{off} = T - t_{on} \quad (21)$$

$$V_o = (2D - 1)V_{DC} \quad (22)$$

iv) PWM Control

As shown in Fig. 11, DC input voltage ( $V_{DC}$ ), supplied by BC, at the input of VSI is measured and compared against the reference voltage given by (13). Produced voltage error ( $V_E$ ) is applied across PI or lead-lag voltage-control compensator for processing. Output of the compensator ( $I_D$ ), being DC in nature, is multiplied by  $\sqrt{2}$  and  $\sin\theta$  to get peak sinusoidal reference current ( $I_D^*$  equal to  $I_{DP}\sin\theta$ ), synchronized with the grid voltage  $V_s$ . The sinusoidal reference current is compared against measured sinusoidal current ( $i_s$ ) and error applied across current-control compensator to track reference current with no or minimal error. Output of the current-control compensator is applied across PWM controller to produce switching sequence for the FB-VSI switches.

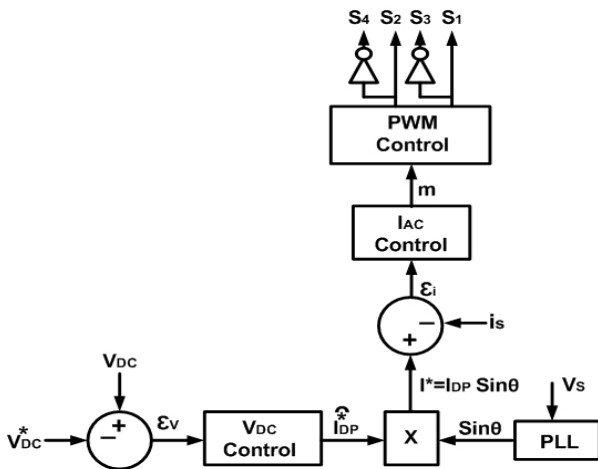


Fig. 11 Maximum power point

V. SIMULATION RESULTS

To evaluate the effectiveness of the proposed model of the AC-PV module directly from datasheet, the model was simulated firstly as an individual AC-PV module, secondly as 675W, 3-AC-PV modules, one across each pair of phases and finally as a 4 kW system. AC-PV module Sunpower E19/240 AC module datasheet is used for modeling.

A. Model as an AC-PV Module

The model of the AC-PV module as a complete unit, producing AC at grid frequency and voltage is connected to the grid. The point of common coupling has a voltage of 208 V<sub>LL</sub> and a frequency of 60 Hz. The proposed AC-PV module model is connected between phases A and B and can supply 225 W of continuous power at max.

Fig. 12 shows  $V_s$ ,  $i_s$  and output power ( $P_o$ ) of the individual AC-PV module model.  $V_s$  equals 208V with peak amplitude of 294V. Current  $i_s$  varies with changes in G and has rms value of 1.08A (225W/208V) with a peak of 1.53A.  $P_o$  equals the reference power ( $P^*$ ) minus loss. From sometime before 5 seconds up to almost 8 seconds the  $P^*$  equals to 240 W (a DC-PV module power at STC); however,  $P_o$  is limited to 225W, the continuous output power of the MI. In Fig. 13 we have zoomed in on a small section of Fig. 12 in order to reveal the

sinusoidal nature of  $V_s$  and  $i_s$  as well as their rms values.

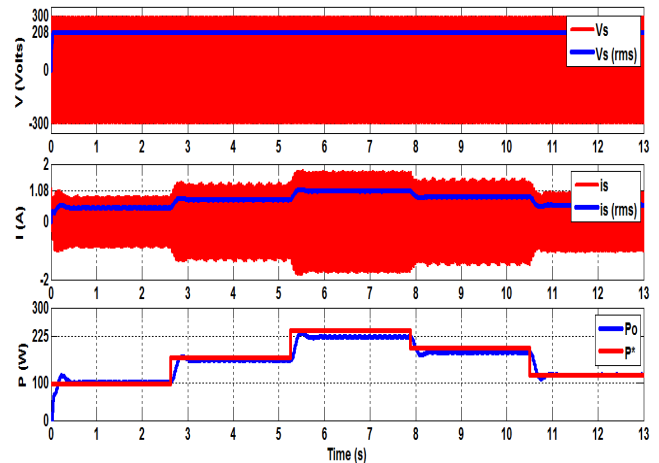


Fig. 12  $V_s$ ,  $i_s$  and  $P_o$  of the AC-PV module model

B. Model as AC-PV Module across Each Pair of Phases

To verify the effectiveness of the proposed AC-PV module model as a part of the system, a 675 W system is connected across the grid at point of common coupling with 208 V<sub>LL</sub> and 60 Hz frequency. AC-PV modules are evenly distributed among the three phases to keep the power system balanced. Thus, one AC-PV module is connected between phases A and B, another one between B and C, and another between C and A. Each AC-PV module produces 225 W of continuous power, thus the total power of the system is  $225 \times 3 = 675$  W.

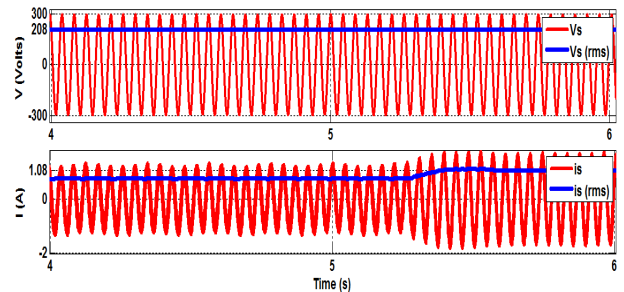


Fig. 13 Zoomed in  $V_s$  and  $i_s$

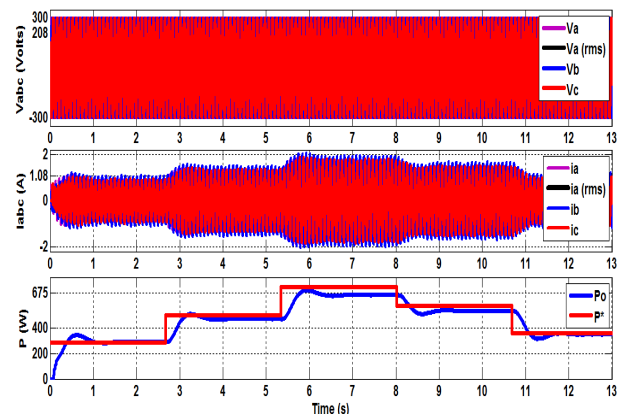


Fig. 14  $V_{abc}$ ,  $i_{abc}$  and  $P_o$  of the 675W AC-PV module model based PV system

Fig. 14 shows  $V_{abc}$ ,  $i_{abc}$  and output power ( $P_o$ ) of the AC-PV module model based PV system.  $V_{LL}$  equals 208V with phase peak amplitude of 294V. Three phase currents,  $i_{abc}$ , vary with changes in G and phase current has rms value of 1.08A with a peak of 1.53A.  $P_o$  equals the reference power ( $P^*$ ) minus loss and varies with changes in G.  $P_o$  equals 675W when  $P^*$  equals 720W at STC.

In Fig. 15 we have zoomed in on a small section of Fig. 14 in order to reveal the sinusoidal nature of  $V_{abc}$  and  $i_{abc}$  as well as their rms values.

### C. Model as 4kW System

Finally, effectiveness of the proposed AC-PV module model as a part of the 4kW system was simulated. As usual AC-PV modules were evenly distributed among the three phases to keep the power system balanced. Thus, 6 AC-PV module were connected between phases A and B, 6 between B and C, and another 6 between C and A. Each AC-PV module produces 225 W of continuous power. Thus the total power of the system was  $225 \times 18 = 4050$  W.

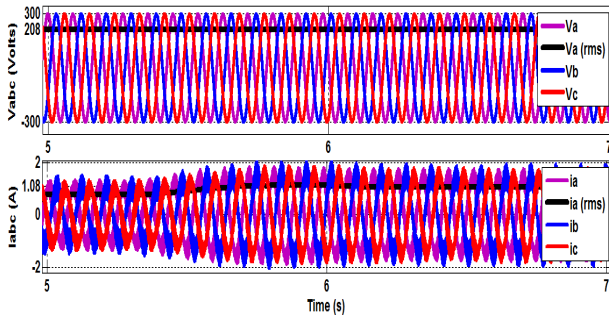


Fig. 15 Zoomed in  $V_{abc}$  and  $i_{abc}$

Fig. 16 shows  $V_a$ ,  $i_a$  and output power ( $P_o$ ) of the AC-PV module model based 4kW PV system. As expected,  $V_{LL}$  equals 208V with phase peak amplitude of 294V. Phase a current ( $i_a$ ) varies with changes in G and phase current has rms value of 1.08A with a peak of 1.53A.  $P_o$  equals the reference power ( $P^*$ ) minus loss and varies with variations in G.  $P_o$  equals 4 kW when  $P^*$  equals 4.3 kW at STC.

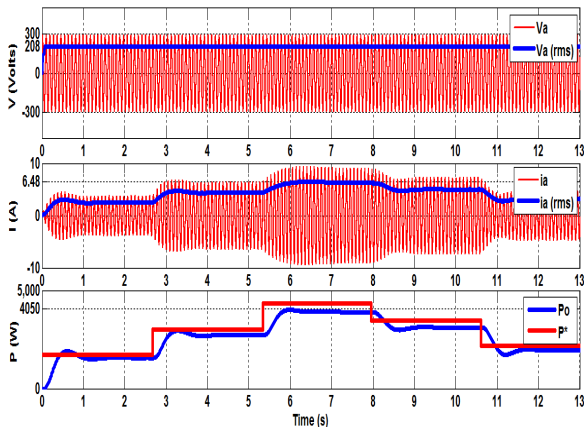


Fig. 16  $V_a$ ,  $i_a$  and  $P_o$  of the 4kW AC-PV module model based PV system

## VI. CONCLUSION

AC-PV module was modeled directly from the data provided by the manufacturer in a datasheet and without using diode equivalent(s) or Shockley equation. Modeling was done on the module level rather than the cell level, treating AC-PV module as a single unit complete system. The proposed model is simple and accurate and yet accounts for the effects of irradiance and temperature. The model was simulated in Matlab/Simulink and simulation results confirmed the model's adequacy.

## REFERENCES

- [1] A. E. Shahat, "PV cell module modeling & ANN Simulation for smart grid applications", Journal of Theoretical and Applied Information Technology, JATIT, (2010).
- [2] S. S. Mohammed "Modeling and Simulation of Photovoltaic module using Matlab/Simulink", International Journal of Chemical and Environmental Engineering, Vol; 2, No.5 (2011).
- [3] M. Katsanevakis, "Modeling the photovoltaic module", International Symposium Industrial Electronics, IEEE, (2011).
- [4] A. Chouder, S. Silvestre, N. Sadaoui and L. Rahmani, "Modeling & simulations of a grid connected PV system based on the evaluation of main PV module parameters", Elsevier, Simulation Modeling Practice and Theory, Vol; 20, Iss; 1, (2012).
- [5] T. Salmi, M. Bouzguenda, A. Gastli and A. Masmoudi, "Matlab/Simulink based modeling of solar photovoltaic cell", International journal of renewable energy research, (2012).
- [6] N. C. Sahoo, I. Elamvazuthi, N.M. Nor, P. Sebastian and B.P. Lim, "PV Panel Modeling using Simscape", Energy, Automation and Signal (ICEAS) International Conference, (2011).
- [7] H. Liang, C. STu, and Y. J. Su, "Development of Generalized Photovoltaic Model using Matlab/Simulink", Proceedings of the World Congress on Engineering and Computer Science, (2008).
- [8] A. Jenifer, N. R. Newlin, G. Rohini, and V. Jamuna, "Development of Matlab/Simulink model for Photovoltaic arrays", International Conference on Computing, Electronics and Electrical Technologies, (2012).
- [9] V. Sangsawang and S. Chaitusaney, "Modeling of Photovoltaic Module from Commercial Specification in Datasheet", Conference of Electrical/Electronics Engineering, Computer, Telecommunications and Information Technology IEEE, (2012).
- [10] D. Sera, R. Teodorescu and P. Rodriguez, "PV panel model based on datasheet values", International Symposium Industrial Electronics IEEE, (2007).
- [11] G. Farivar and B. Assaei, "Photovoltaic module single diode model parameters extraction based on manufacturer datasheet parameters", International conf. on pow. & energy, IEEE, (2010).
- [12] I. M. Syed and A. Yazdani, "Simple Mathematical Model of Photovoltaic Module for Simulation in Matlab/Simulink", Canadian Conf. on Elec. and Computer Engineering, IEEE, (2014).